

Autodisplay: One-Component System for Efficient Surface Display and Release of Soluble Recombinant Proteins from *Escherichia coli*

JOCHEN MAURER,¹ JOACHIM JOSE,² AND THOMAS F. MEYER^{1,2*}

Abteilung Infektionsbiologie, Max-Planck-Institut für Biologie, 72076 Tübingen,¹ and Abteilung Molekulare Biologie, Max-Planck-Institut für Infektionsbiologie, 10117 Berlin,² Germany

Received 26 August 1996/Accepted 24 September 1996

The immunoglobulin A protease family of secreted proteins are derived from self-translocating polyprotein precursors which contain C-terminal domains promoting the translocation of the N-terminally attached passenger domains across gram-negative bacterial outer membranes. Computer predictions identified the C-terminal domain of the *Escherichia coli* adhesin involved in diffuse adherence (AIDA-I) as a member of the autotransporter family. A model of the β -barrel structure, proposed to be responsible for outer membrane translocation, served as a basis for the construction of fusion proteins containing heterologous passengers. Autotransporter-mediated surface display (autodisplay) was investigated for the cholera toxin B subunit and the peptide antigen tag PEYFK. Up to 5% of total cellular protein was detectable in the outer membrane as passenger autotransporter fusion protein synthesized under control of the constitutive P_{TK} promoter. Efficient presentation of the passenger domains was demonstrated in the outer membrane protease T-deficient (*ompT*) strain *E. coli* UT5600 and the *ompT dsbA* double mutant JK321. Surface exposure was ascertained by enzyme-linked immunosorbent assay, immunofluorescence microscopy, and immunogold electron microscopy using antisera specific for the passenger domains. In strain UT2300 (*ompT*⁺), the passenger domains were released from the cell surface by the OmpT protease at a novel specific cleavage site, R ↓ V. Autodisplay represents a useful tool for future protein translocation studies with interesting biotechnological possibilities.

Bacterial surface display of recombinant proteins is a promising tool for the analysis of macromolecular interactions. Possible applications include the production of (i) immunoglobulin variable chains with distinct specificities, (ii) receptors or ligands for binding studies, (iii) antigenic determinants for vaccine development and (iv) peptide libraries for epitope mapping or antibody specificity tests (46). For application (iv), phage display libraries, especially filamentous phage harboring coat proteins with surface-exposed N-terminal domains which tolerate foreign peptide inserts (8), have been extensively used. In contrast to such well-established phage systems, bacterial display systems possess the advantage of being self-replicative, thus enabling direct multiplication of cells and stringent selection for a desired binding phenotype. In addition, bacterial display systems, in contrast to phage, exhibit a strict genotype phenotype linkage, which is crucial for stringent phenotypic selections.

The autotransporter-containing polyprotein precursors of the immunoglobulin A1 (IgA1) protease-like family of secreted proteins (21) are excellent candidates for surface display of heterologous passenger proteins in gram-negative bacteria. The primary translational products of these proteins consist of a signal peptide at the N terminus, one or several domains to be transported, and an autotransporter structure at the C terminus. The autotransporter domain forms, after translocation through the cytoplasmic membrane, a barrel of 14 amphipathic β -sheets within the outer membrane. Through the aid of this porin-like structure, the N-terminally attached passenger proteins are translocated to the surface (34). In the

case of IgA1 protease from *Neisseria gonorrhoeae*, the most extensively investigated member of this protein family, the passenger domains are autoproteolytically cleaved off the transporter domain (25). However, this feature is not common to all autotransporter-containing proteins (21). The autotransporter of IgA1 protease from *N. gonorrhoeae* (similar IgA proteases are also expressed by *N. meningitidis* and *Haemophilus influenzae* [35]) has been used to transport heterologous passenger domains to the surfaces of *Salmonella typhimurium* and *Escherichia coli* (23, 24). Proteins to be secreted by this pathway must maintain in an unfolded state in the periplasm since outer membrane translocation is blocked by stable tertiary structures formed by disulfide bonds (26). Consistently, the *E. coli* periplasmic oxidoreductase DsbA, responsible for the formation of disulfide bonds (2), is not essential in the autotransporter pathway and affects the translocation of cysteine-containing passengers negatively (22, 24). The cell surface-directed protease OmpT of *E. coli* was used for the release of heterologous passenger proteins to the medium (24, 44). While this may be desirable for certain applications, an *E. coli dsbA ompT* double mutant that allowed export and stable display of a cysteine-containing passenger on the *E. coli* cell surface was constructed (22).

AIDA-I, an *E. coli* adhesin involved in diffuse adherence to HeLa cells, was recently cloned and genetically characterized (4). Although a second gene, *orfA*, was required for expression of the diffuse adherence phenotype, the *aida* gene appeared to be sufficient for surface exposure of AIDA-I in the recombinant host (6). The gene product of *orfA* was assumed to post-translationally modify AIDA-I since coexpression of *orfA* resulted in an increased apparent molecular weight of AIDA-I (5).

With the goal to establish an efficient autotransporter system

* Corresponding author. Mailing address: Max-Planck-Institut für Biologie, Abteilung Infektionsbiologie, Spemannstr. 34, 72076 Tübingen, Germany. Phone: 49-70 71-601-221. Fax: 49-70 71-61 03 79.

derived from *E. coli* as a native host, we assessed the feasibility of the putative autotransporter domain of AIDA-I for translocation of heterologous passenger proteins across the outer membrane. Here we demonstrate efficient autodisplay in *E. coli* of two different passengers, the ~13-kDa cholera toxin B subunit (CTB) and the peptide antigen tag PEYFK.

MATERIALS AND METHODS

Bacterial strains. *E. coli* UT2300 (F⁻ *ara-14 leuB6 azi-6 lacY1 proC14 tsx-67 entA403 trpE38 rfbD1 rpsL109 xyl-5 mlr-1 thi1*) and UT5600 (UT2300 Δ ompT-*lepC266*) (strain collection numbers E149 and E151) have been described elsewhere (10). *E. coli* Sure (E154) was obtained from Stratagene Cloning Systems. Enteropathogenic *E. coli* (EPEC) 2787 (E180) was kindly provided by H. K. Geiss, Hygieneinstitut, Universität Heidelberg. The construction of *E. coli* JK321 (Δ ompT *proC leu-6 trpE38 ent zih12::Tn10 dsbA::kan*) (E177) has been described elsewhere (22). For all purposes, bacteria were routinely grown at 37°C on Luria-Bertani agar plates containing 50 mg of ampicillin liter⁻¹.

Recombinant DNA techniques. The autotransporter domain including a sufficient linking region was amplified from a plasmid preparation of EPEC 2787 by PCR using the primers JM1 (5'-GGAAGATCTGCCTCAGAAATGAGGGCC-3') JM7 (5'-CGGGTACCCTTAATCCTACAAAAGAAAGT-3'). JM1 and JM7 contained *Bgl*II and *Kpn*I sites, respectively. The PCR product was cleaved with *Bgl*II and *Kpn*I. Plasmid pTK61 (23) was used as a template for PCR with primers JM6 (5'-CATGGTACCAGGCGTTTATTATTCCTAC-3') and EF16 (5'-TGTAACACGACGGCCAGTATCACGAGGCCCTTCGT-3'), and the resulting PCR product, encoding a mutant CTB protein without cysteines (24), was cleaved with *Kpn*I and *Clal*. In a triple ligation, both PCR fragments obtained were inserted into pBA vector DNA previously cleaved with *Bam*HI and *Clal*.

For the construction of pJM22, primers JM7 and JM20 (5'-AAGGGTACCTTTGAAATACTCCGGAGTAATATTTGAGGTGTC-3'), both containing *Kpn*I restriction sites, were used to amplify pJM7 DNA including the signal sequence of CTB but no additional *ctxB*-derived sequences. The 5' extension of JM20 encoded five amino acids (PEYFK) that are recognized as a linear epitope by monoclonal antibody Dü142 (42). The PCR product was digested with *Kpn*I and circularized to yield pJM22.

Preparation of plasmid DNA, ligations, restriction digestions, transformation procedures, and DNA electrophoresis were performed according to common procedures (35). Ligation products were initially transformed into *E. coli* Sure and then transferred to other strains. Enzymes used in this study were obtained from Applied Gene Technology Systems, New England Biolabs, Boehringer Mannheim, and Pharmacia.

In vivo techniques. For whole-cell protease treatments, *E. coli* cells were collected from agar plates, suspended in phosphate-buffered saline (PBS), and adjusted to an optical density at 578 nm (OD₅₇₈) of 10.0. To 0.2 ml of cell suspension, 2 μ l of protease stock solution was added to yield a final concentration of 50 mg of chymotrypsin or trypsin liter⁻¹. Suspensions were incubated for 20 min at 37°C, and digestion was stopped by washing the cells three times with 750 μ l of PBS containing 10% fetal calf serum (FCS). Cells were sedimented by brief centrifugation and suspended either in PBS for immunofluorescence and electron microscopy studies or in sample buffer (29) and boiled immediately for 15 min for sodium dodecyl sulfate (SDS)-polyacrylamide gel electrophoresis (PAGE) and Western blotting.

For the assessment of OmpT-dependent release of protein domains, *E. coli* UT2300(pJM7) and UT5600(pJM7) were collected from agar plates and suspended in PBS to yield an OD₅₇₈ of 10.0. Suspensions were vortexed for 20 s and centrifuged for 5 min at 13,000 \times g. Clarified supernatants were diluted 1:2 with 2 \times sample buffer and boiled for 10 min, and 10 μ l was subjected to SDS-PAGE and Western blotting.

Immunolabeling. For immunofluorescence studies, cells were collected as described for whole-cell enzyme-linked immunosorbent assay (ELISA). In a 24-well cell culture plate, 50 μ l of the cell suspension was spread on circular coverslips (15 mm in diameter) and fixed by adding 450 μ l of 2.5% paraformaldehyde for 20 min. After three washes with 500 μ l of PBS, blocking was performed by addition of 300 μ l of PBS plus 1% FCS per well for 5 min. Blocking solution was completely aspirated, and 15 μ l of primary antibody per well was applied to the coverslips. After prolonged incubation for 1 h at room temperature in a humidified box, the reaction was stopped by three washes with PBS. The procedure for applying the second antibody (goat anti-rabbit or anti-mouse conjugated to Texas red) was identical to that for the primary antibody except that we used three 15-min washes with PBS. Coverslips were placed on microscope slides, and samples were evaluated by fluorescence microscopy (23).

For immunogold labeling, antisera AK55 and Dü142 were used in 1:100 and 1:17 dilutions, respectively. Bacteria were pipetted onto Formvar-coated copper grids and fixed with PBS-2.5% paraformaldehyde for 10 min. After three washes with PBS, blocking was performed for 10 min with PBS-10% FCS. Grids were then placed on drops of primary antibody containing PBS-10% FCS for 45 min. After being washed three times, the primary antibody was labeled with protein A-5-nm gold (PAG10; 1:50 in PBS-10% FCS; Biocell Research Laboratories) applied under the conditions described for the primary antibody. After incubation

with protein A-gold, copper grids were washed four times with distilled water and results were evaluated by electron microscopy (23).

For whole-cell ELISA, cells were collected from plates and suspended in PBS to a final OD₅₇₈ of 1. Each well of a 24-well cell culture plate (Multidish; Nunc) was coated with 50 μ l of cell suspension. For cell attachment, plates were incubated for 12 h at 37°C. Blocking was carried out for 1 h with 150 μ l of PBS-10% FCS. Following aspiration of the blocking solution, cells were incubated with 100 μ l of primary antibody for 45 min at 37°C. Anti-CTB (AK55) was diluted 1:200 in PBS-10% FCS, while anti-PEYFK (Dü142) was diluted 1:35 in PBS-10% FCS. Plates were washed four times with 150 μ l of PBS per well. Protein A (Sigma, Deisenhofen, Germany) was diluted 1:500 in PBS, and 100 μ l of this solution was applied to each well for 30 min. Cells were washed four times with 150 μ l of PBS, and subsequently 100 μ l of 4-nitrophenylphosphate (1 g liter⁻¹) in 100 mM ethanolamine was added per well. The reaction was stopped after 15 to 25 min by adding 50 μ l of 3 M NaOH. Results were determined as OD₄₀₅ values.

Differential fractionation of *E. coli*. *E. coli* cells grown overnight at 37°C were collected from agar plates and suspended in PBS to yield an OD₅₇₈ of 5.0. The suspension was passed through a French pressure cell at 960 lb/in² once to lyse the bacteria. The lysate was centrifuged at 5,000 \times g for 10 min to remove intact bacteria and large debris. The clarified bacterial lysate was centrifuged for 30 min at 100,000 \times g, and the resulting supernatant contained proteins from the periplasm and cytoplasm. The pellet was suspended in PBS-1% sarcosyl (*N*-lauryl sarcosinate, sodium salt) and centrifuged for 30 min at 100,000 \times g. The supernatant contained proteins of the cytoplasmic membrane, while pelleted proteins were derived from the outer membranes.

Protein preparation and N-terminal amino acid sequencing. SDS-PAGE and Western blotting were carried out as described previously (34). Fragments derived from whole-cell digestion with either trypsin or chymotrypsin or from degradation by OmpT of FP59 and FP50 were copurified with outer membranes and subjected to SDS-PAGE. The proteins were electrotransferred to a polyvinylidene difluoride membrane (Trans-Blot; Bio-Rad). Protein bands were stained with Coomassie brilliant blue R250. The respective bands were excised. Microsequencing by automated Edman chemistry was performed with an ABI 477A protein sequencer (Applied Biosystems).

RESULTS

Secondary structure prediction. Structure prediction of the C-terminal domain of the AIDA-I precursor was performed by using the FORTRAN program AMPHI (20, 46). This program is highly adapted for the prediction of amphipathic β -sheets within membranes. It was successfully used in predicting the structure of OmpF (46) before crystal data were available. An amphipathic β -strand is predicted if the hydrophobicity $H\beta(i)$ varies within a period of two residues by $H\beta(i) \geq 0.6$ and $H\beta(i+1) \leq 0.4$ (20a), where the underlying equation is $H\beta(i) = [h(i \pm 4) + h(i \pm 2) + h(i)]/5$. This method predicts the AIDA-I precursor to be an autotransporter containing an outer membrane-embedded C-terminal domain. The autotransporter domain comprises 14 antiparallel, amphipathic β -sheets spanning amino acids positions 1003 to 1286 of the AIDA-I precursor (Fig. 1A). These results were confirmed by calculating regions of high surface probability as described by Emini et al. (11), using the GCG program from the Wisconsin sequence analysis package (9). Such regions are assumed to be incompatible with transmembrane strands (Fig. 1A). Analogous to known porin crystal structures (28, 37), the last membrane-spanning β -sheet is predicted to run from the cell surface to the C-terminal end, directed to the periplasm. Consequently, the antiparallel first β -sheet of the barrel runs from the periplasm to the surface. This suggests a periplasmic location of attached passengers prior to outer membrane translocation. However, an additional transmembrane loop is predicted to be necessary for the translocation of the unfolded passenger across the outer membrane (34). The known porin crystal structures exhibit membrane-spanning β -sheets that are slightly inclined toward the vertical of the membrane (30). A model of the AIDA-I autotransporter domain was constructed in accordance with this finding by minimizing the number of charged amino acids directed toward membrane-exposed parts of the β -barrel (Fig. 1B).

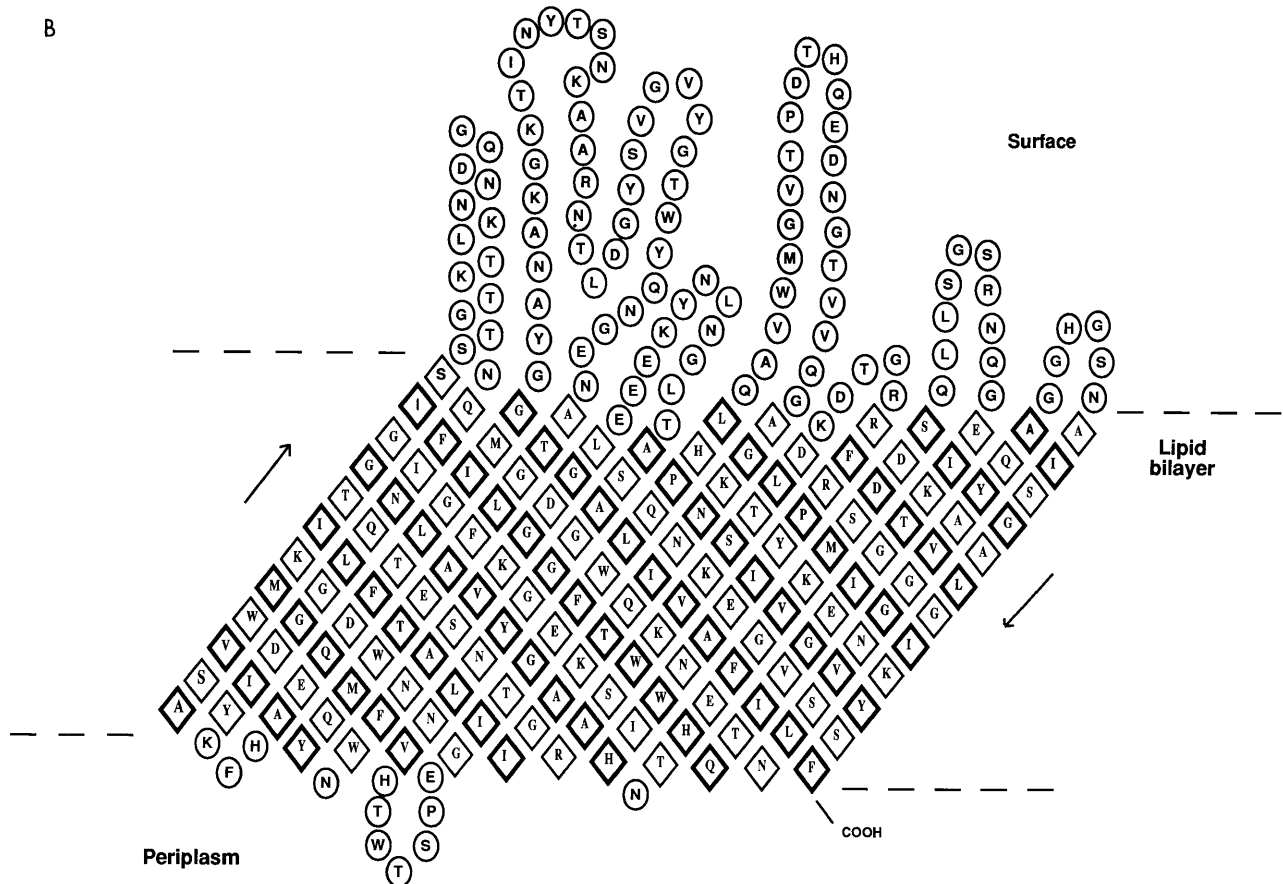
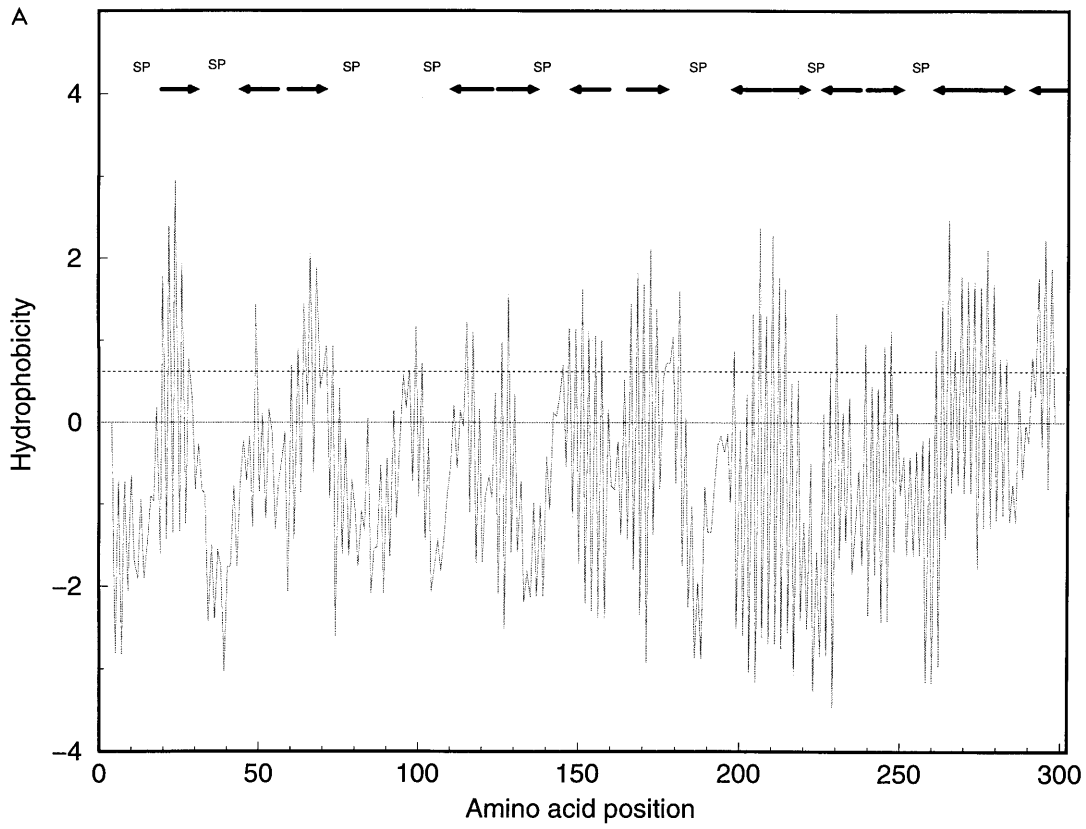


FIG. 1. Modeling of the AIDA-I autotransporter β -barrel by amphipathic β -sheet prediction. (A) Hydrophobicity plot of the C-terminal 300 amino acids of AIDA-I based on the computer program AMPHI (20). The solid line marks the limit of hydrophobicity that must be obtained by at least one amino acid within a predicted amphipathic transmembrane β -sheet (20a). Arrows pointing to the right indicate transmembrane regions running from the surface to the periplasmic side of the outer membrane; arrows pointing to the left indicate the opposite orientation of the transmembrane β -strands. Regions of high surface probability (SP) were calculated as described by Emini et al. (11) by the aid of the GCG sequence analysis package (10). (B) Hypothetical topology of the AIDA-I β -barrel. Locations of amino acids (one-letter code) within the outer membrane are indicated by diamonds; circles indicate non-membrane-embedded regions. Amino acids in boldface diamonds are hydrophobic according to the AMPHI analysis and therefore presumably directed to the membrane-exposed part of the β -barrel structure. Amino acids in lightface diamonds are hydrophilic according to AMPHI and should face the interior. The β -barrel-like structure is completed by interaction of the first transmembrane strand with the antiparallel C-terminal one (arrows). The β -barrel structure starts with the alanine at position 1003 according to the published AIDA-I amino acid sequence (5 [accession number X65022]).

Construction of recombinant fusion protein-encoding genes. To determine whether the predicted autotransporter domain of AIDA-I was sufficient for outer membrane translocation, two different passenger domains were chosen as reporters. CTB was employed because it was used previously as a passenger protein in secretion experiments with the IgA1 protease autotransporter (23, 24). The use of CTB fusions therefore allows a direct comparison between the IgA1 protease and AIDA-I autotransporter systems with regard to the efficiency of the surface display in *E. coli*. To avoid hindrance of passenger translocation by disulfide bond formation in the periplasm, a mutated CTB lacking cysteine residues was chosen. The modified CTB protein is ~ 12.8 kDa in size including the signal sequence. The respective gene was PCR amplified by using plasmid pTK61 as the

template (23). pTK61 is a pBR322-derived medium-copy-number plasmid that directs the expression of the CTB-IgA β fusion protein B61 under control of the constitutive P_{TK} promoter. The AIDA-I autotransporter domain, including a linker region, that was sufficient for export was PCR amplified by using the ~ 100 -kb plasmid carrying the *aida-I* gene of EPEC 2787 (4) as a template. The amplified gene fragments were fused in frame and inserted into a high-copy-number derivative of vector pBR322 under control of the constitutive P_{TK} promoter (23). The fusion protein encoded by the resulting plasmid, pJM7, was termed FP59 on the basis of its predicted molecular mass of 58.9 kDa (Fig. 2). Export of FP59 was assessed in several different *E. coli* host strains.

As an additional passenger, we chose the peptide antigen tag PEYFK, which is ~ 1.7 kDa in size (Fig. 2) and recognized by

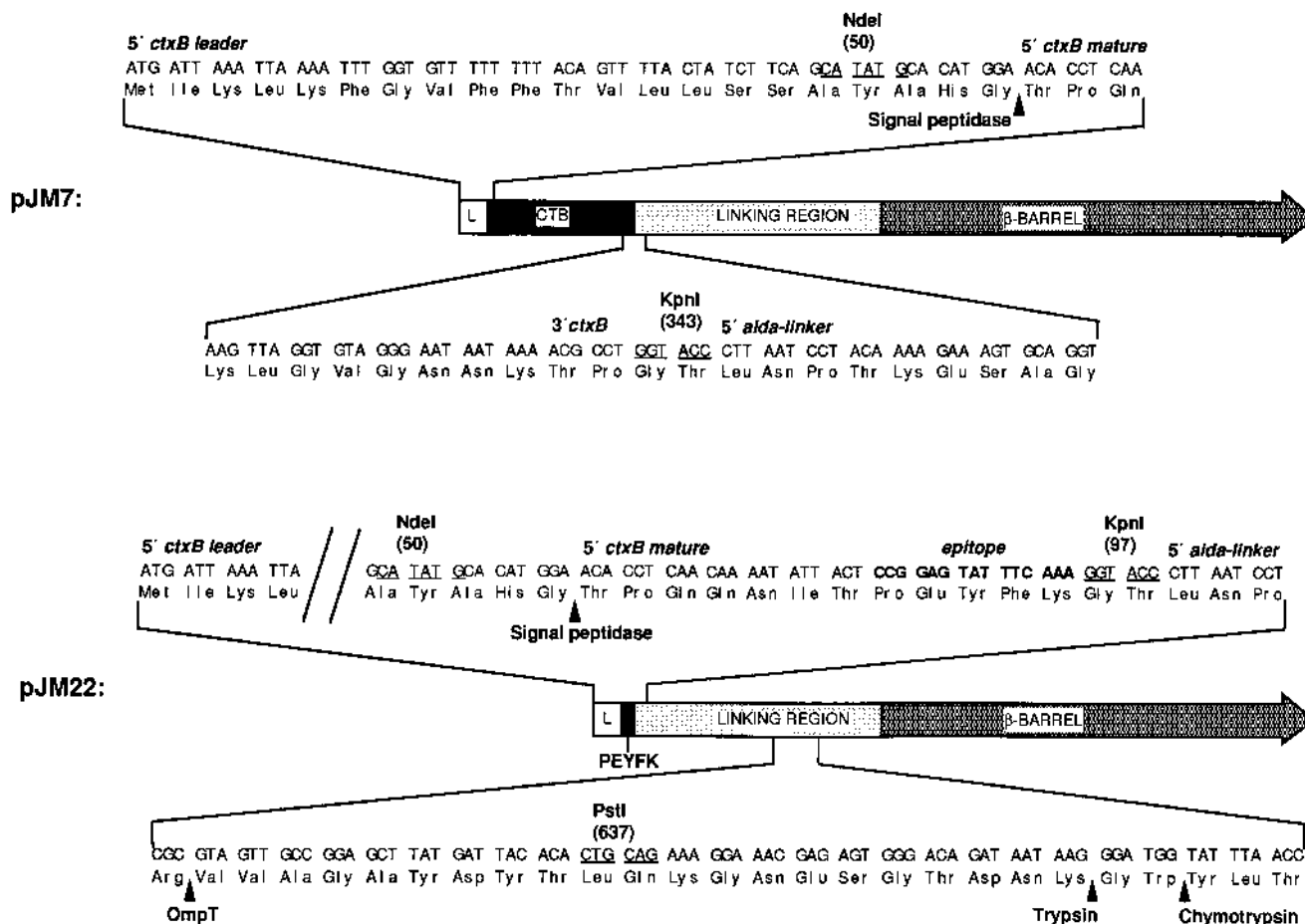


FIG. 2. Structures of the fusion proteins FP59 and FP50. The environments of the fusion sites of FP59 (pJM7) and FP50 (pJM22) are given as sequences. The protease cleavage sites are marked within the AIDA-I autotransporter, and the linking regions and β -barrels are indicated.

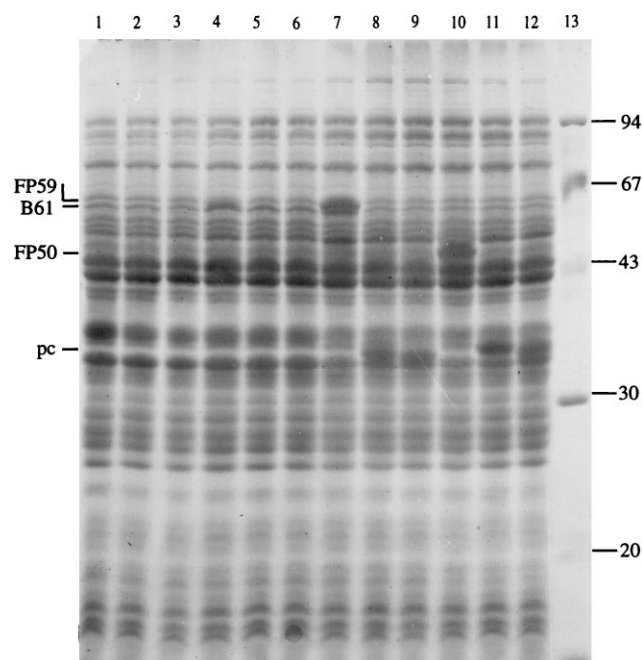


FIG. 3. Identification of plasmid-encoded gene products B61, FP59, and FP50 by SDS-PAGE. Cells of *E. coli* UT5600 (*ompT*) harboring either pTK1 encoding native periplasmic CTB (lanes 1 to 3), pTK61 encoding the IgA_β-CTB fusion B61 (lanes 4 to 6), pJM7 encoding the AIDA_β-CTB fusion FP59 (lanes 7 to 9), or pJM22 encoding the PEYFK-AIDA_β fusion FP50 (lanes 10 to 12) were left undigested (lanes 1, 4, 7, or 10) or digested with trypsin (lanes 2, 5, 8, and 11) or chymotrypsin (lanes 3, 6, 9, and 12). The positions of size markers (lane 13) are indicated in kilodaltons at the right; positions of fusion proteins B61, FP59, and FP50 are shown at the left. pc, protease-resistant cores resulting from trypsin or chymotrypsin digestion of FP59 or FP50.

monoclonal antibody Dü142 (42). For this purpose, we constructed plasmid pJM22, which encodes fusion protein FP50 exhibiting a molecular mass of 49.7 kDa (Fig. 2). FP50 and FP59 both contained the portion of the AIDA-I precursor comprising the C-terminal 446 amino acids, accounting for ~48.1 kDa.

Surface expression and external protease accessibility. *E. coli* UT5600 (*ompT*) was used for transformation with plasmids pJM7 and pJM22. From previous work with the IgA1 protease autotransporter (24) and also another exported protein (18), the *E. coli* outer membrane protease OmpT is known to cleave surface-exposed passenger proteins. Therefore, strain UT5600 was useful to prevent the possible cleavage of surface-displayed regions in FP50 and FP59. The expression of the fusion proteins was initially monitored by SDS-PAGE of whole-cell lysates. As shown in Fig. 3, FP59 and FP50 were easily detectable by Coomassie brilliant blue staining of crude or partially enriched cell lysates. Both fusion proteins were visualized as prominent protein bands, migrating in agreement with their predicted molecular masses of 58.9 and 49.8 kDa, respectively, representing up to 5% of the total cellular protein.

Physiologically intact bacteria expressing FP59 or FP50 were subjected to protease digestion with trypsin and chymotrypsin. As shown by SDS-PAGE of whole-cell lysates and subsequent staining with Coomassie blue, the digestion resulted in the disappearance of the full-size fusion proteins and generated lower-molecular-weight products, representing protease-resistant membrane-embedded cores (Fig. 3). As described in Materials and Methods, the trypsin-resistant outer membrane-

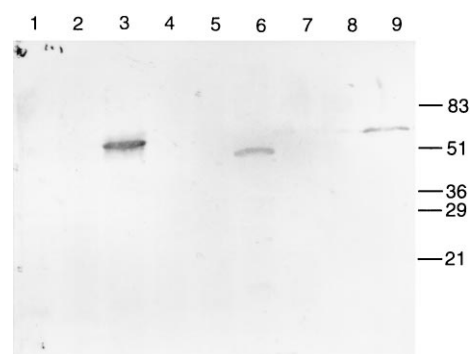


FIG. 4. Protease treatment and immunoblotting of fusion proteins produced in strain UT5600 (*ompT*). Fusion proteins analyzed are FP59 (CTB-AIDA_β fusion; lanes 1 to 3), FP50 (PEYFK-AIDA_β fusion; lanes 4 to 6), and B61 (IgA_β-CTB fusion; lanes 7 to 9). Lysates in lanes 1, 4, and 7 were digested with trypsin; those in lanes 2, 5, and 8 were digested with chymotrypsin; those in lanes 3, 6, and 9 were undigested controls. The immunoblot was developed with anti-CTB serum AK55 and monoclonal antibody Dü142. Positions of molecular mass markers are given in kilodaltons at the right.

associated core of FP59 was subjected to N-terminal sequence analysis, revealing the sequence GWYLT. This sequence corresponds to amino acids 225 to 229 of the fusion protein FP59 (Fig. 2) and to amino acids 948 to 952 in the AIDA-I precursor (5). The trypsin cleavage site is located 54 amino acids upstream of the N terminus of the predicted AIDA β-barrel structure and confirms the trypsin cleavage site K ↓ G. In contrast, the trypsin cleavage sites R ↓ Q and R ↓ P located 13 and 16 amino acids downstream of G⁹⁴⁸ were not cleaved, indicating they were protected by the membrane-embedded part of the autotransporter. The molecular mass of the trypsin resistant core was calculated to be 37.1 kDa, which is in agreement with the observed molecular mass after SDS-PAGE (Fig. 3).

Similarly, the accessibility of chymotrypsin cleavage sites was assessed. Site W ↓ Y between positions 226 and 227 of FP59 was found to be cleaved. The next consensus chymotrypsin cleavage sites, between positions 227 and 228 or 228 and 229, however, were not processed, indicating that this region of the linker was not accessible for chymotrypsin (Fig. 2). This finding suggests that the predicted AIDA-I β-core requires an additional linker region of at least 52 amino acids in order to support complete surface display of an N-terminally attached passenger.

Digested and undigested whole-cell lysates containing FP50 and FP59 were subjected to Western blot analysis after SDS-PAGE, using either AK55, a polyclonal rabbit anti-CTB serum, or monoclonal antibody Dü142. By this method, CTB or PEYFK fusions were detected only in undigested lysates, while digestion with trypsin and chymotrypsin caused degradation of the immunoreactive domains in FP59 and FP50 (Fig. 4). This result demonstrated the surface accessibility of the N termini in both fusion proteins.

Native CTB was shown to oligomerize, forming pentamers with high affinity (32). *E. coli* UT5600, as well as JK321 cells, expressing FP59 were found to clump in solution. Cell clusters were partially disrupted by excessive vortexing for more than 1 min. After 10 to 20 min of prolonged incubation at room temperature, clustering of cells was restored. However, clustering was prevented after digestion of FP59-expressing cells with trypsin or chymotrypsin. With cells expressing FP50, such clustering was not observed. This result suggested that the exported CTB domain was responsible for the clustering phenomenon. While we do not expect expression of G_{M1}-specific adherence of the surface displayed CTB domain because of the

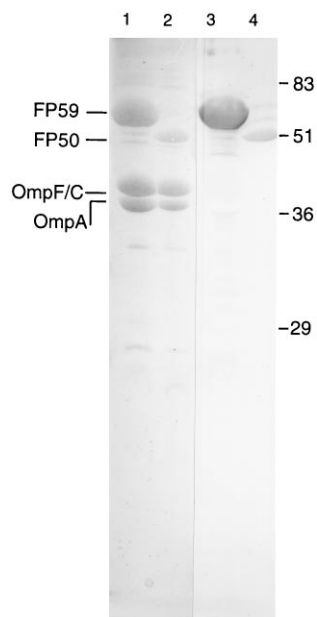


FIG. 5. Outer membrane localization of FP59 (CTB-AIDA_B fusion) and FP50 (PEYFK-AIDA_B fusion). Outer membranes prepared from a 1-ml culture were separated by SDS-PAGE (17.5% gel). Gels were either stained with Coomassie brilliant blue (lanes 1 and 2) or immunoblotted (lanes 3 and 4) with anti-CTB serum AK55 and monoclonal antibody Dü142. Lanes 1 and 3, outer membrane preparations from *E. coli* UT5600(pJM7) encoding FP59; lanes 2 and 4, outer membrane preparations from *E. coli* UT5600(pJM22) encoding FP50. Positions of molecular mass markers are given in kilodaltons at the right.

lack of several essential C-terminal amino acids (24), the surface-exposed domain might still favor subunit-subunit interactions.

To determine whether the outer membrane integrity was influenced by the AIDA-I autotransporter-containing fusion proteins, OmpA was used as a control in Western blot experiments. OmpA, naturally located within the outer membrane of *E. coli*, is known to possess a trypsin-susceptible periplasmic moiety at the C terminus (27). Therefore, trypsin-digested whole cells expressing FP50 and FP59 were analyzed for stability of OmpA. If the periplasm was accessible for trypsin, the size of OmpA should be reduced by approximately 10 kDa owing to degradation of the C terminus. However, none of the recombinant *E. coli* strains producing FP59 or FP50 exhibited signs of OmpA degradation by trypsin, whereas OmpA was readily degraded in osmotically shocked cells (data not shown). This finding indicated that autotransporter-mediated transport of recombinant passenger domains did not interfere with outer membrane integrity and that the fusion proteins were degraded by trypsin from outside.

Membrane fractions and soluble fractions from *E. coli* UT5600 harboring pJM7 or pJM22 were prepared by the sarcosyl method (12) to confirm the outer membrane location of FP59 and FP50. Western blot analysis showed that the soluble fraction, consisting of cytoplasmic and periplasmic proteins, as well as the sarcosyl-soluble membrane fraction, representing the cytoplasmic membrane, contained only minor amounts of FP59 and FP50, respectively (not shown). In the sarcosyl-insoluble fraction corresponding to the outer membrane, three dominant protein bands were readily detectable in Coomassie blue-stained gels (Fig. 5). Besides the nonseparated double band consisting of OmpF and OmpC (39 kDa) and the OmpA (36 kDa) band, we detected a third prominent band represent-

ing the fusion FP59 or FP50. This result indicated the stable membrane integration of the FP59 and FP50 core regions.

OmpT-dependent release of surface-exposed passenger protein. The *E. coli* outer membrane protease OmpT is known to cleave proteins at the bacterial cell surface (14, 24). To determine whether surface-exposed parts of FP59 and FP50 could be cleaved by OmpT, plasmids pJM7 and pJM22 were propagated in *E. coli* UT2300 (*ompT*⁺). Western blot analysis of whole-cell lysates of *E. coli* UT2300 harboring either pJM7 or pJM22 revealed only minute quantities of the full-size fusion protein FP59 or FP50, respectively (Fig. 6a; compare lanes 1 and 2, 3 and 4, and 5 and 6). Both fusion proteins were processed completely by OmpT, giving rise to a common protease-resistant core (Fig. 6b). The protease-resistant core was not labeled in Western blots but could be detected on Coomassie blue-stained SDS-polyacrylamide gels. The core proteins therefore no longer contained the passenger epitopes recognized by the AK55 and Dü142 antibodies (Fig. 6a and b). Additionally, outer membrane preparations of UT2300(pJM7) and UT2300(pJM22) exhibited the same OmpT-resistant core proteins.

OmpT cores from FP50 and FP59 were subjected to N-terminal sequence determination by Edman degradation. The N-terminal sequence VVAGAY was identical in both products. This motif corresponds to amino acids 122 to 127 of FP50 and to amino acids 204 to 209 of FP59. The sequence R↓V represents a new, previously undescribed cleavage site of OmpT (43). The calculated molecular mass of the remaining OmpT-resistant outer membrane-embedded core was 39.6 kDa. This was in good agreement with its observed molecular mass of ~42 kDa in SDS-PAGE. No additional OmpT-generated fragments were detected despite the presence of several classical OmpT cleavage sites further downstream in FP50 and FP59. Also, one classical OmpT site present in CTB was earlier shown to be resistant to cleavage (24). The epitope tag PEYFK does not contain any classical OmpT cleavage sites.

The fate of the immunogenic domain released to the supernatant by OmpT protease activity on FP59 was further investigated. *E. coli* UT2300(pJM7) cells were washed in buffer, and cell-free wash supernatants were analyzed by Western blotting. Supernatants contained a protein with a molecular mass of approximately 18 kDa. This is in good agreement with the calculated molecular mass of 19.6 kDa of the domain released from FP59 at the cleavage site R↓V, indicating that OmpT released the surface-exposed domain into the supernatant (Fig. 6c). Therefore, OmpT cleavage must have taken place at the intact bacterial cell surface. The released protein domain was, however, not further degraded by OmpT.

Next we attempted to show that cleavage by intrinsic or externally added proteases does not affect the association of protease-resistant cores in the outer membrane. For this purpose, outer membranes were prepared from untreated OmpT-positive *E. coli* UT2300(pJM7) and UT2300(pJM22) and also from the OmpT-negative *E. coli* UT5600(pJM7) and UT5600(pJM22) expressing full-size fusion proteins FP59 and FP50, respectively. In addition, whole cells of *E. coli* UT5600(pJM7) and UT5600(pJM22) treated with either trypsin or chymotrypsin were used to prepare outer membranes. Outer membrane proteins were analyzed by SDS-PAGE followed by Coomassie blue staining. As shown in Fig. 7, the protease-resistant cores remained stably incorporated in the outer membrane irrespective of the processing with either trypsin, chymotrypsin, or OmpT. Notably, no difference in the quantity of protease-resistant cores was seen for cleavage by externally added proteases versus cell-associated OmpT protease. FP50 and FP59 were expressed in amounts similar to

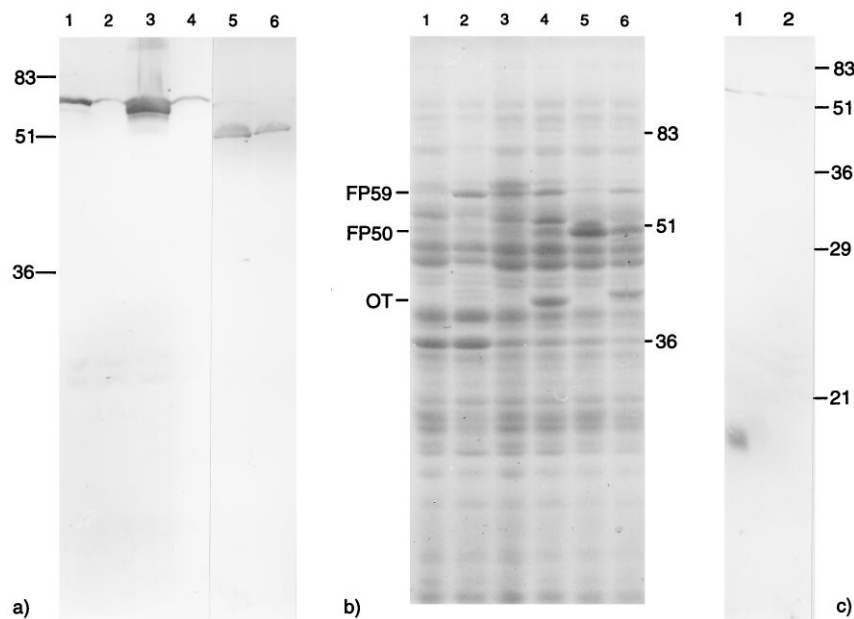


FIG. 6. OmpT-dependent release of surface exposed domains of FP59 and FP50. (a) Western blot of *E. coli* UT5600 (*ompT*) (lanes 1, 3, and 5) and *E. coli* UT2300 (*ompT*⁺) (lanes 2, 4, and 6) harboring pTK61 encoding the Iga_β-CTB fusion B61 (lanes 1 and 2), pJM7 encoding the AIDA_β-CTB fusion FP59 (lanes 3 and 4), or pJM22 encoding the PEYFK-AIDA_β fusion FP50 (lanes 5 and 6). Immunoblotting was performed with anti-CTB serum AK55 and PEYFK-specific monoclonal antibody Dü142. Positions of molecular mass marker proteins are indicated in kilodaltons at the left. (b) Coomassie blue staining of whole-cell lysates. Lanes are identical to those in panel A. Positions of molecular mass marker proteins are indicated in kilodaltons at the right. OT, the OmpT-processed membrane-associated portions of FP59 and FP50. (c) Supernatant detection of the OmpT-released domain from FP59. Supernatants were prepared as described in Materials and Methods and analyzed by SDS-PAGE (17.5% gel). Lane 1, *E. coli* UT2300 (*ompT*⁺)(pJM7); lane 2, *E. coli* UT5600 (*ompT*)(pJM7). Positions of molecular mass standards are indicated in kilodaltons at the right.

those of the major outer membrane proteins OmpA and OmpC/F. The strong expression of FP50 or FP59 did not significantly affect the quantities of OmpA and OmpC/F present in the outer membrane (data not shown).

Immunolabeling of surface-exposed proteins. Immunolabeling with specific antibodies or antisera is a potent tool to detect surface-exposed proteins. Three different methods were applied to demonstrate the surface exposure of passenger proteins exported by AIDA_β: (i) whole-cell ELISA, allowing the quantification of surface-exposed antigens; (ii) indirect immunofluorescence microscopy; and (iii) indirect immunogold labeling.

The OmpT-negative *E. coli* UT5600(pJM7) and UT5600(pJM22), expressing FP59 and FP50, respectively, were first analyzed by whole-cell ELISA. *E. coli* UT5600 harboring the pBA vector without an insert was used as a control to determine the system-dependent background. The efficiency of the AIDA-I autotransporter-mediated surface display was compared with that of the CTB-Iga_β fusion B61 encoded by the previously described plasmid pTK61 (24). UT5600 cells bearing the different plasmids were analyzed with antibody AK55. For every strain, the mean values of three independent quadruplicate experiments were determined. pBA vector-derived background was subtracted from each value, and the highest value in each experiment obtained with pJM7 was set to 100%. As shown in Fig. 8, the AIDA-I autotransporter-mediated surface display of the CTB passenger was substantially more efficient than Iga_β-mediated surface display. The anti-CTB serum AK55 did not show any significant reaction with the PEYFK-AIDA_β fusion protein FP50 produced by UT5600(pJM22), indicating that this serum was specific for CTB.

E. coli UT5600 cells harboring plasmid pTK1, pTK61, pJM7,

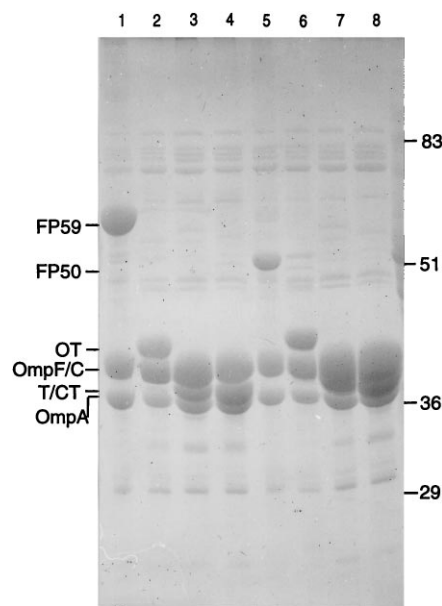


FIG. 7. Subcellular location of the protease-resistant β -cores of FP59 and FP50. *E. coli* UT5600 (*ompT*) harboring either pJM7 encoding the AIDA_β-CTB fusion FP59 or pJM22 encoding the PEYFK-AIDA_β fusion FP50 were treated with trypsin or chymotrypsin or left untreated as a control. *E. coli* UT2300 (*ompT*⁺)(pJM7) and UT2300 (pJM22) were used as additional controls without protease treatment. Outer membranes were prepared as described in Materials and Methods, and proteins were analyzed by SDS-PAGE (13% gel) and Coomassie blue staining. Lane 1, *E. coli* UT5600 (*ompT*)(pJM7); lane 2, *E. coli* UT2300 (*ompT*⁺)(pJM7); lane 3, *E. coli* UT5600 (*ompT*)(pJM7), trypsin treated; lane 4, *E. coli* UT5600(pJM7), chymotrypsin treated; lane 5, *E. coli* UT5600 (pJM22); lane 6, *E. coli* UT2300(pJM22); lane 7, *E. coli* UT5600(pJM22), trypsin treated; lane 8, *E. coli* UT5600(pJM22), chymotrypsin treated. Positions of molecular mass markers are given in kilodaltons at the right. OT, OmpT-resistant core; T/CT, trypsin- and chymotrypsin-resistant cores.

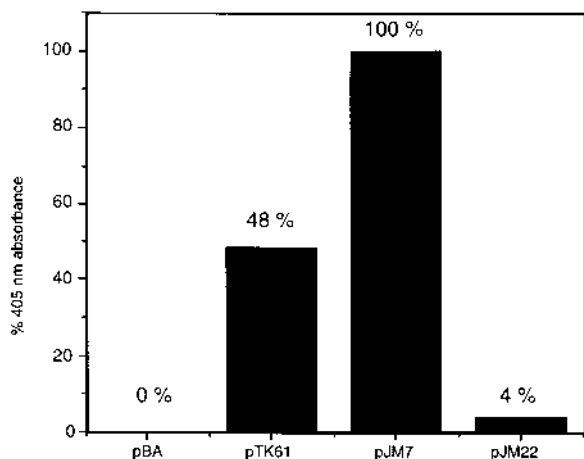


FIG. 8. Whole-cell ELISA of *E. coli* UT5600 harboring either pBA, pTK61, pJM7, or pJM22. Values are means of three independent quadruplet measurements. Extinction was measured at 405 nm in 3-min intervals, and the reaction was usually stopped after 10 to 20 min by addition of 3 M NaOH.

or pJM22 were subjected to indirect immunofluorescence labeling, using either AK55 or Dü142 and a goat anti-rabbit or anti-mouse Texas red conjugate as the secondary antibody. Plasmid pTK1 expressing periplasmic CTB (23) was used as a negative control. Bacteria containing pTK61 (encoding the CTB-IgA_B fusion B61) or pJM7 (encoding the CTB-AIDA_B fusion FP59) but not pTK1 or pJM22 (encoding the PEYFK-AIDA_B fusion FP50) were positively stained when incubated with anti-CTB serum AK55. In contrast, *E. coli* UT5600 (pJM22), but not UT5600(pJM7), was found to be positive when assayed with monoclonal antibody Dü142 (Fig. 9). In an additional experiment, UT5600(pJM7) cells were protease treated, washed, and mixed at different ratios with untreated cells. The mixtures were subsequently subjected to indirect immunofluorescence. The intensity of labeling was found to strictly correspond with the given ratio of untreated cells, thus indicating that immunofluorescence depended only on antibody recognition of the surface-exposed domains (data not shown).

Immunogold labeling of strains expressing antigens produced results similar to those obtained by immunofluorescence labeling. *E. coli* UT5600 cells expressing B61 bound 20 to 25 gold particles per cell on average, whereas those expressing FP59 bound 40 to 45 gold particles per cell when AK55 and protein A-gold conjugates were used. Minimal label was observed for *E. coli* UT5600(pTK1) cells synthesizing the periplasmic form of CTB (zero to three gold particles per cell), and the same result was obtained with *E. coli* UT5600(pJM22), expressing FP50 when assayed with AK55. The reciprocal experiment with the peptide-specific Dü142 yielded 40 to 45 gold particles per cell for *E. coli* UT5600(pJM22) and 0 to 3 particles per cell of *E. coli* UT5600(pJM7).

The same experiments performed with *E. coli* UT5600 were also performed with the *dsbA ompT* double-mutant strain JK321 (22). For all plasmids investigated, results were essentially identical (data not shown).

DISCUSSION

The data presented in this study clearly demonstrate that AIDA-I is a member of the autotransporter family of secreted proteins, as previously predicted (21). Insertion of the auto-

transporter domain in the outer membrane of *E. coli* was accompanied by resistance to exogenous and endogenous protease treatment. No special accessory factors were necessary to support the autotransporter function of AIDA-I in the investigated host strains. The autotransporter function was used for the efficient secretion of two heterologous passengers. Autodisplay could be demonstrated by passenger-specific antibody binding as well as by the protease-mediated release of the passenger domains into the supernatant. The efficiency of secretion was significantly improved in comparison to previously developed systems, e.g., IgA1 protease-mediated autodisplay (23).

On the basis of several structural commonalities, the IgA1 protease-like autotransporters have been defined as a novel family of secreted proteins (21). The most striking feature of these proteins is the ability of the C-terminal part to form a β -barrel within the outer membrane. This β -barrel consists of amphipathic, antiparallel β -sheets and enables the translocation of N-terminal covalently attached passengers to the surface. Thus far, all members of this family of secreted proteins have been associated with pathogenic species. In addition to the 10 members listed by Jose et al. (21), the SepA protein of *Shigella flexneri* (3), the SpaP protein of *Rickettsia prowazekii* (7), a 120-kDa outer membrane protein of *R. rickettsii* (13), the SlpT protein of *R. typhi* (17), and two additional neisserial polyproteins besides IgA1 protease (our unpublished data) most likely belong to the family of autotransporters. Some members, such as IcsA from *S. flexneri* (33), are surface-attached proteins; other autotransporters, like the IgA1 proteases of *Neisseria* species and *H. influenzae* (34, 35) and the VacA protein of *Helicobacter pylori* (38), release their passenger domains into the supernatant. This processing can occur autoproteolytically as in the case of IgA1 protease or might be facilitated by independent surface-associated bacterial host proteases, such as OmpT (24).

Previous work of this laboratory focused on the autotransporter function of IgA1 protease from *N. gonorrhoeae*. Several *E. coli* mutant strains employed in this study were used here to investigate the translocation function of the AIDA-I protein (4). In contrast to IgA1 protease, this protein occurs naturally in *E. coli* (21) and therefore was considered a superior tool for export studies in this homologous host. Initially, we constructed a model of the AIDA-I β -barrel based on a structure prediction approach. In analogy to the outer membrane porins for which crystal data are available, the N-terminal β -strand of the barrel structure is assumed to run from the periplasm to the surface. Therefore, for complete surface exposure of a passenger domain, an additional linker region is required. Based on this model, fusion proteins consisting of the AIDA β -barrel, a linker region, and two different passengers were constructed. Both passengers were transported to the outer membrane of the *E. coli* hosts. The exported passengers could be detected by specific antibodies, indicating their proper translocation across the outer membrane. The fusion proteins were expressed, in some instances, at levels exceeding that of the resident outer membrane proteins OmpF and OmpC, yet the outer membrane remained intact, as confirmed by the protease resistance of the periplasmic domain of OmpA. The application of the externally added proteases trypsin and chymotrypsin and the surface-associated *E. coli* protease OmpT led to either the complete destruction or release of the passenger domains, thus indicating correct folding and function of the AIDA-I autotransporter.

OmpT is known to cleave secreted fusion proteins and thereby allows harvesting of the mature products from the culture supernatant (1, 18, 24). The N-terminal amino acid

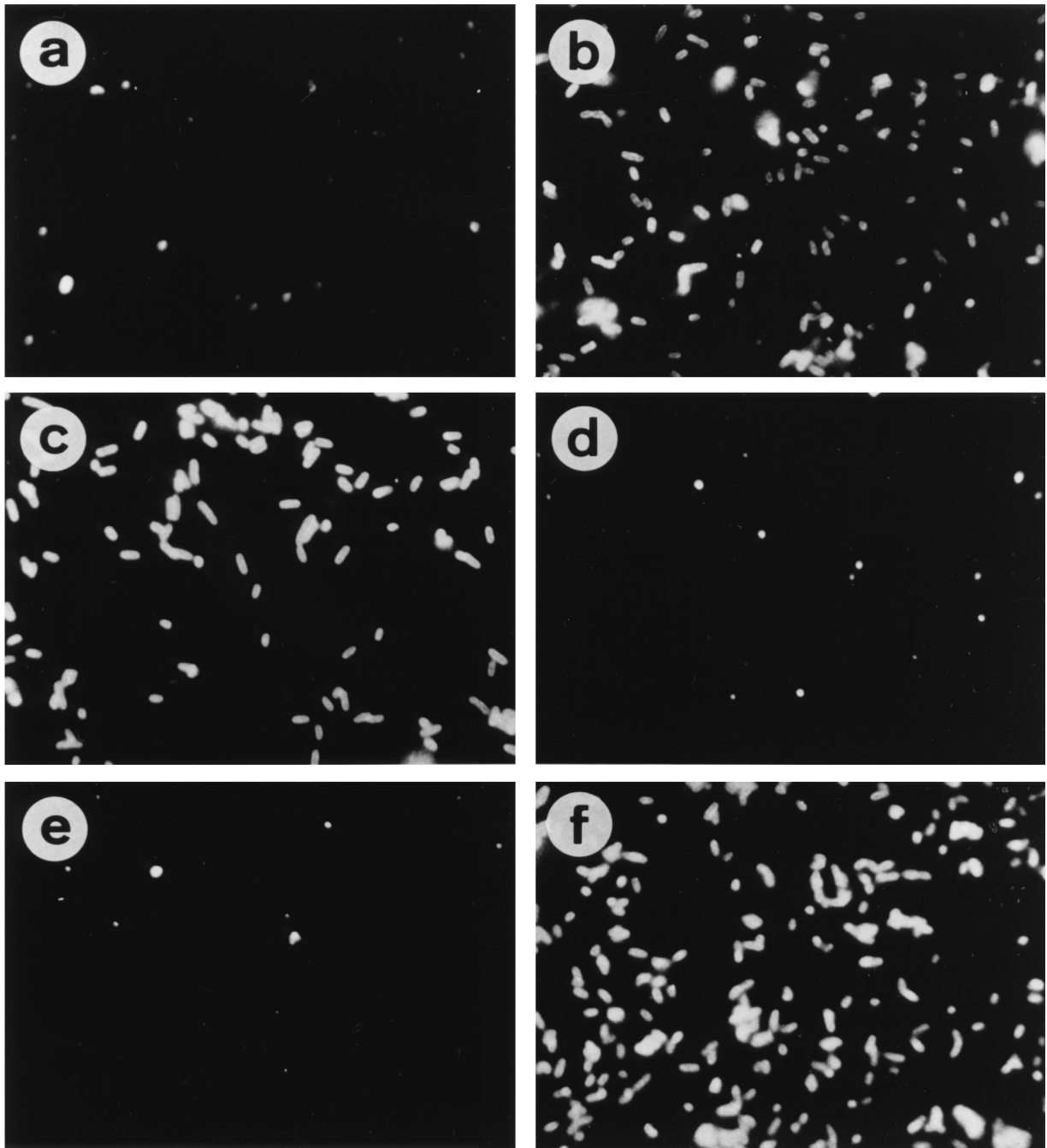


FIG. 9. Immunofluorescence of *E. coli* UT5600 (*ompT*) harboring various plasmids. (a) pTK1 encoding native periplasmic CTB; (b) pTK61 encoding the CTB-IgA_β fusion B61; (c and e) pJM7 encoding the CTB-AIDA_β fusion FP59; (d and f) pJM22 encoding the PEYFK-AIDA_β fusion FP50. Immunofluorescent bacteria in panels a through d were labeled with anti-CTB serum AK55; those in panels e and f were labeled with monoclonal antibody Dü142 (anti-PEYFK).

sequences of the protease-resistant cores which remained in the outer membrane were analyzed. The cleavage sites were identical for both passenger constructs and found to be located within the linker regions of the fusions. The sequencing data fully confirmed our topology model of the AIDA-I β -barrel as well as the concept of the translocation mechanism, which is, however, still rudimentary (Fig. 10).

Interestingly, the CTB passenger contained an internal OmpT cleavage site which was resistant to cleavage by OmpT, as it was in similar approaches with the IgA1 autotransporter

(24). This might indicate the acquisition of a stable conformation of the exported passenger. Alternatively, the OmpT activity might be restricted to the proximity of the bacterial cell surface. Similarly, several potential cleavage sites within the predicted β -barrel were recognized by neither extraneous nor endogenous proteases. This finding supports the idea that the membrane embedding of the β -barrel prevents accessibility to proteases. Notably, previous studies on the processing of the natural 132-kDa AIDA-I precursor revealed no cleavage by OmpT (4–6). Therefore, further investigations will be neces-

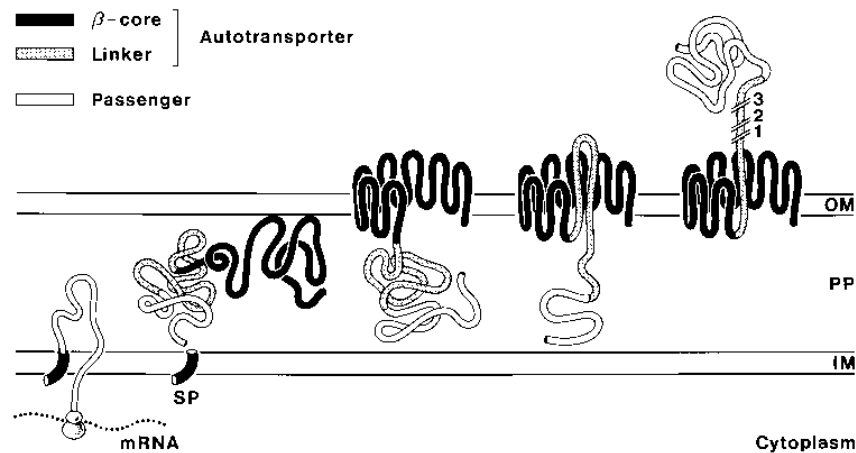


FIG. 10. Model of autodisplay by the AIDA-I autotransporter. The nascent peptide chain of native AIDA-I or recombinant fusions with the C-terminal AIDA-I autotransporter is translocated across the inner membrane (IM) via the Sec-dependent pathway. As the C-terminal core domain arrives in the periplasm (PP), it assembles as a β -barrel in the outer membrane (OM), generating a translocation pore for the N-terminally attached linker region and the passenger domain. Hydration and conformational energy may be the driving force for the protein translocation across the outer membrane. Cleavage sites of chymotrypsin (1), trypsin (2), and OmpT (3) within the linker region of the AIDA-I autotransporter are marked. SP, signal peptide.

sary to gain more insight into the processing of native AIDA-I precursor.

This study included a comparison between two different autotransporters for which *E. coli* represented either a homologous or a heterologous host system. Expression of the AIDA-I fusions was tolerated at a substantially higher level than expression of Iga β fusions. In this context, it is worth noting that in preliminary experiments, the AIDA-I autotransporter-mediated secretion of several other passenger proteins had no significant influence on growth rate or spontaneous lysis of *E. coli* host cells (our unpublished data). The AIDA-I fusion proteins could be visualized by Coomassie blue staining of protein gels, which was not possible in the heterologous system (24, 31, 41). Several attempts to construct a high-copy-number plasmid containing an Iga β -CTB fusion failed, suggesting toxicity of the construct. Reasons accounting for this failure might be a decreased compatibility of the heterologous β -barrels in the *E. coli* outer membrane. However, even in the case of the VirG autotransporter in its homologous host *S. flexneri*, visualization of heterologous fusion proteins required immunostaining (44). Western blotting was necessary to detect all autotransporter fusion proteins studied thus far, with the exception of the AIDA-I fusions reported here.

Future applications of the AIDA-I autodisplay system are possible in several areas. One important area concerns the construction of efficacious live recombinant bacterial vaccines. Recent evidence suggests a superior efficacy of secreted antigens over somatic antigens in protection experiments (19). The AIDA-I autotransporter could be an efficient means to export antigens of interest without impairing the vaccine strain stability. Furthermore, proteins of enzymes of biotechnological interest could be secreted and functionally displayed on the *E. coli* cell surface. The only known limitation of autodisplay is the formation of stable tertiary structures of the passengers in the periplasm, as previously revealed with the Iga β autodisplay system (24). This is because outer membrane translocation requires an unfolded passenger conformation. However, stabilization of tertiary structures by cysteine bridging can be efficiently circumvented in an oxidoreductase-negative (*dsbA*) mutant (21). Therefore, cysteine-containing proteins can be surface displayed under appropriate conditions. An interesting feature of autodisplay is the option of releasing exported pas-

sengers into the medium by the action of the host cell OmpT protease or, alternatively, by addition of site-specific proteases, such as IgA1 protease (39). This optional feature may prove advantageous for the screening of display libraries. The AIDA-I autotransporter is therefore anticipated to be a promising tool for advancement of modern display technology.

ACKNOWLEDGMENTS

We thank L. Shi and P. Wernet for providing us with monoclonal antibody D \ddot{u} 142, R. Spohn and G. Jung for communicating the target sequence of D \ddot{u} 142, and H. K. Geiss providing EPEC 2787. We are grateful to D. Stoll for performing the N-terminal sequence analysis and to Y. D. Stierhof for the generous gift of antiserum K57. In particular, we thank J. Mellies for critically reading the manuscript and also K. Lamberty for the artwork.

REFERENCES

- Baneyx, F., and G. Georgiou. 1990. In vivo degradation of secreted fusion proteins by the *Escherichia coli* outer membrane protease OmpT. *J. Bacteriol.* **172**:491–494.
- Bardwell, J. C., K. McGovern, and J. Beckwith. 1991. Identification of a protein required for disulfide bond formation in vivo. *Cell* **67**:581–589.
- Benjelloun-Touimi, Z., P. J. Sansonetti, and C. Parsot. 1995. Characterization of SepA, the major extracellular protein of *Shigella flexneri*: autonomous secretion and involvement in tissue invasion. *Mol. Microbiol.* **17**:123–135.
- Benz, I., and M. A. Schmidt. 1989. Cloning and expression of an adhesin (AIDA-I) involved in diffuse adherence of enteropathogenic *Escherichia coli*. *Infect. Immun.* **57**:1506–1511.
- Benz, I., and M. A. Schmidt. 1992. AIDA-I, the adhesin involved in diffuse adherence of the diarrhoeagenic *Escherichia coli* strain 2787 (O126:H27), is synthesized via a precursor molecule. *Mol. Microbiol.* **6**:1539–1546.
- Benz, I., and M. A. Schmidt. 1993. Diffuse adherence of enteropathogenic *Escherichia coli* strains—processing of AIDA-I. *Zentralbl. Bakteriol.* **278**:197–208.
- Carl, M., W.-M. Ching, M. E. Dobson, and G. A. Dasch. 1990. Characterization of the gene encoding the protective paracrystalline-surface-layer protein of *Rickettsia prowazekii*: presence of a truncated identical homolog in *Rickettsia typhi*. *Proc. Natl. Acad. Sci. USA* **87**:8237–8241.
- Clackson, T., H. Hoogenboom, A. D. Griffiths, and G. Winter. 1991. Making antibody fragments using phage display libraries. *Nature* **352**:624–628.
- Devereux, J., P. Haeberli, and O. Smithies. 1984. A comprehensive set of sequence analysis programs for the VAX. *Nucleic Acids Res.* **12**:387–395.
- Elish, M. E., J. R. Pierce, and C. F. Earhart. 1988. Biochemical analysis of spontaneous *fepA* mutants of *Escherichia coli*. *J. Gen. Microbiol.* **134**:1355–1364.
- Emimi, E. A., J. V. Hughes, D. S. Perlow, and J. Boger. 1985. Induction of hepatitis A virus-neutralizing antibody by a virus-specific synthetic peptide. *J. Virol.* **55**:836–839.

12. Filip, C., G. Fletcher, J. L. Wulff, and C. F. Earhart. 1973. Solubilization of the cytoplasmic membrane of *Escherichia coli* by the ionic detergent sodium-lauryl sarcosinate. *J. Bacteriol.* **115**:717–722.
13. Gilmore, R. D., Jr., W. Cieplak, Jr., P. F. Policastro, and T. Hackstadt. 1991. The 120 kilodalton outer membrane protein (rOmp B) of *Rickettsia rickettsii* is encoded by an unusually long open reading frame: evidence for protein processing from a large precursor. *Mol. Microbiol.* **5**:2361–2370.
14. Grodberg, J., and J. J. Dunn. 1988. OmpT encodes the *Escherichia coli* outer membrane protease that cleaves T7 RNA polymerase during purification. *J. Bacteriol.* **170**:1245–1253.
15. Grodberg, J., and J. J. Dunn. 1989. Comparison of *Escherichia coli* K-12 outer membrane protease OmpT and *Salmonella typhimurium* E protein. *J. Bacteriol.* **171**:2903–2905.
16. Gunneriusson, E., P. Samuelson, M. Uhlen, P.-A. Nygren, and S. Stahl. 1996. Surface display of a functional single-chain Fv antibody on staphylococci. *J. Bacteriol.* **178**:1341–1346.
17. Hahn, M. J., K. K. Kim, I. Kim, and W. H. Chang. 1993. Cloning and sequence analysis of the gene encoding the crystalline surface layer protein of *Rickettsia typhi*. *Gene* **133**:129–333.
18. Hanke, C., J. Hess, G. Schumacher, and W. Goebel. 1992. Processing by OmpT of fusion proteins carrying the HlyA transport signal during secretion by the *Escherichia coli* hemolysin transport system. *Mol. Gen. Genet.* **233**:42–48.
19. Hess, J., I. Gentshev, D. Miko, M. Welzel, C. Ladel, W. Goebel, and S. H. E. Kaufmann. 1996. Superior efficacy of secreted over somatic antigen display in recombinant *Salmonella* vaccine induced protection against listeriosis. *Proc. Natl. Acad. Sci. USA* **93**:1458–1463.
20. Jähnig, F. 1990. Structure predictions of membrane proteins are not that bad. *Trends Biochem. Sci.* **15**:93–95.
- 20a. Jähnig, F. Personal communication.
21. Jose, J., F. Jähnig, and T. F. Meyer. 1995. Common structural features of IgA1 protease-like outer membrane protein autotransporters. *Mol. Microbiol.* **18**:377–382.
22. Jose, J., J. Krämer, T. Klausner, J. Pohlner, and T. F. Meyer. 1996. Absence of periplasmic DsbA oxidoreductase facilitates export of cysteine-containing passenger proteins to the *Escherichia coli* cell surface via the IgA₂ autotransporter pathway. *Gene* **178**:107–110.
23. Klausner, T., J. Pohlner, and T. F. Meyer. 1990. Extracellular transport of cholera toxin B subunit using *Neisseria* IgA protease β -domain: conformation-dependent outer membrane translocation. *EMBO J.* **9**:1991–1999.
24. Klausner, T., J. Pohlner, and T. F. Meyer. 1992. Selective extracellular release of cholera toxin B subunit by *Escherichia coli*: dissection of *Neisseria* IgA₂-mediated outer membrane transport. *EMBO J.* **11**:2327–2335.
25. Klausner, T., J. Pohlner, and T. F. Meyer. 1993. The secretion pathway of IgA protease-type proteins in gram-negative bacteria. *Bioessays* **15**:799–805.
26. Klausner, T., J. Krämer, K. Otzelberger, J. Pohlner, and T. F. Meyer. 1993. Characterization of the *Neisseria* IgA₂-core. The essential unit for outer membrane targeting and extracellular protein secretion. *J. Mol. Biol.* **234**:579–593.
27. Klose, M., A. Störiko, Y. D. Stierhof, I. Hindennach, B. Mutschler, and U. Henning. 1993. Membrane assembly of the outer membrane protein OmpA of *Escherichia coli*. *J. Biol. Chem.* **268**:25664–25670.
28. Kreusch, A., G. E. Schulz. 1994. Refined structure of the porin from *Rhodospseudomonas blastica*. *J. Mol. Biol.* **243**:891–905.
29. Laemmli, U. K. 1970. Cleavage of structural proteins during the assembly of the head of bacteriophage T4. *Nature* **227**:680–685.
30. LaLonde, J. M., D. A. Bernlohr, and L. J. Banaszak. 1994. The up-and-down β -barrel proteins. *FASEB J.* **8**:1240–1247.
31. Li, L. J., G. Dougan, P. Novotny, and I. G. Charles. 1991. P.70 pertactin, an outer-membrane protein from *Bordetella parapertussis*: cloning, nucleotide sequence and surface expression in *Escherichia coli*. *Mol. Microbiol.* **5**:409–417.
32. Ludwig, D. S., R. K. Holmes, and G. K. Schoolnik. 1985. Chemical and immunochemical studies on the receptor binding domain of cholera toxin B subunit. *J. Biol. Chem.* **260**:12528–12534.
33. Nakata, N., T. Tobe, I. Fukuda, T. Suzuki, K. Komatsu, M. Yoshikawa, and C. Sasakawa. 1993. The absence of a surface protease, OmpT, determines the intercellular spreading ability of *Shigella*: the relationship between the ompT and kcpA loci. *Mol. Microbiol.* **9**:459–468.
34. Pohlner, J., R. Halter, K. Beyreuther, and T. F. Meyer. 1987. Gene structure and extracellular secretion of *Neisseria gonorrhoeae* IgA protease. *Nature* **325**:458–462.
35. Poulsen, K., J. Reinholdt, and M. Kilian. 1992. A comparative genetic study of serologically distinct *Haemophilus influenzae* type 1 immunoglobulin A1 proteases. *J. Bacteriol.* **174**:2913–2921.
36. Sambrook, J., E. F. Fritsch, and T. Maniatis. 1989. *Molecular cloning: a laboratory manual*, 2nd ed. Cold Spring Harbor Laboratory Press, Cold Spring Harbor, N.Y.
37. Schirmer, T., T. A. Keller, Y.-F. Wang, and J. P. Rosenbusch. 1995. Structural basis for sugar translocation through maltoporin channels at 3.1 Å resolution. *Science* **267**:512–514.
38. Schmitt, W., and R. Haas. 1994. Genetic analysis of the *Helicobacter pylori* vacuolating cytotoxin: structural similarities with the IgA protease type of exported protein. *Mol. Microbiol.* **12**:307–319.
39. Schnappinger, D., W. Geissdorfer, C. Sizemore, and W. Hillen. 1995. Extracellular expression of native human anti-lysozyme fragments in *Staphylococcus carnosus*. *FEMS Microbiol. Lett.* **129**:121–127.
40. Schorr, J., B. Knapp, E. Hundt, H. A. Küpper, and E. Amann. 1991. Surface expression of malarial antigens on *Salmonella typhimurium*: induction of serum antibody response upon oral vaccination of mice. *Vaccine* **9**:675–681.
41. Shimada, K., Y. Ohnishi, S. Hirinouchi, and T. Beppu. 1994. Extracellular transport of pseudoazurin of *Alcaligenes faecalis* in *Escherichia coli* using the COOH-terminal domain of *Serratia marcescens* serine protease. *J. Biochem.* **116**:327–334.
42. Spohn, R., F. O. Gombert, and G. Jung. 1992. B-cell epitopes of the Nef protein. *Res. Virol.* **143**:70–72.
43. Sugimura, K., and T. Nishihara. 1988. Purification, characterization, and primary structure of *Escherichia coli* protease VII with specificity for paired basic residues: identity of protease VII and OmpT. *J. Bacteriol.* **170**:5625–5632.
44. Suzuki, T., M. C. Lett, and C. Sasakawa. 1995. Extracellular transport of VirG protein in *Shigella*. *J. Biol. Chem.* **270**:30874–30880.
45. Van der Ley, P., H. Amesz, J. Tommassen, and B. Lugtenberg. 1988. Monoclonal antibodies directed against the cell-surface-exposed part of PhoE pore protein of the *Escherichia coli* K-12 outer membrane. *Eur. J. Biochem.* **147**:401–407.
46. Vaughan, T. J., J. A. Williams, K. Pritchard, J. K. Osbourn, A. R. Pope, J. C. Earnshaw, J. McCafferty, R. A. Hodits, J. Wilton, and K. S. Johnson. 1996. Human antibodies with sub-nanomolar affinities isolated from a large non immunized phage display library. *Nat. Biotechnol.* **14**:309–314.
47. Vogel, H., and F. Jähnig. 1986. Models for the structure of outer membrane proteins of *Escherichia coli* derived from Raman spectroscopy and prediction methods. *J. Mol. Biol.* **190**:191–199.